The generalized active space concept for the relativistic treatment of electron correlation. III. Large-scale configuration interaction and multiconfiguration self-consistent-field four-component methods with application to UO2

Fleig, T.; Jensen, H.J.; Olsen, J.; Visscher, L.

published in
Journal of Chemical Physics
2006

DOI (link to publisher)
10.1063/1.2176609

document version
Publisher's PDF, also known as Version of record

The generalized active space concept for the relativistic treatment of electron correlation. III. Large-scale configuration interaction and multiconfiguration self-consistent-field four-component methods with application to UO_2

Timo Fleig[a)]
Institute of Theoretical and Computational Chemistry, Heinrich Heine University Düsseldorf, Universitätsstraße 1, D-40591 Düsseldorf, Germany

Hans Jørgen Aa. Jensen
Department of Chemistry, University of Southern Denmark, DK-5230 Odense M, Denmark

Jeppe Olsen
Theoretical Chemistry, Aarhus University, Langelandsgade 140, DK-8000 Århus C, Denmark

Lucas Visscher
Department of Theoretical Chemistry, Free University of Amsterdam, De Boelelaan 1083, NL-1081 HV Amsterdam, The Netherlands

(Received 14 October 2005; accepted 23 January 2006; published online 10 March 2006)

We present an implementation for large-scale relativistic electronic structure calculations including spin-dependent contributions and electron correlation in a fully variational procedure. The modular implementation of the double group configuration interaction (CI) program into a multiconfiguration self-consistent-field (MCSCF) code allows for the treatment of large CI expansions in both the spinor optimization step and the post-MCSCF dynamic electron correlation step. As an illustration of the potential of the new code, we calculate the spectroscopic properties of the UO_2 molecule where we study the ground state and a few excited states in vertical and adiabatic calculations.
 [DOI: 10.1063/1.2176609]

I. INTRODUCTION

A number of interesting problems in heavy-element chemistry require accurate descriptions of electron correlation, both static and dynamic, and relativistic contributions, both scalar and spin orbit. Examples are open-shell systems of heavy *p*, *d*, and *f* elements[1–3] and excited states of molecules with closed-shell ground states, for example, in uranyl[4] and coinage metal dimers.[5] Ideally, all of these contributions should be treated on the same footing and, where appropriate, simultaneously. The simultaneous treatment of static electron correlation and spin-orbit coupling is possible with the recently presented four-component Kramers-restricted relativistic multiconfiguration self-consistent-field (KR-MCSCF) implementation[6] based on the theoretical framework in Ref. 7. In the same theoretical framework, a relativistic configuration interaction (CI) program has been presented[8] based on the Dirac-Coulomb Hamiltonian and capable of treating long configuration expansions which aim at the simultaneous treatment of dynamic electron correlation and spin-orbit coupling. The use of configuration expansions of adequate size has, however, often not been possible with the initial KR-MCSCF implementation.

The objective of this paper is to present the combination of these two methods in a dual sense. First, the modular incorporation of the large-scale CI program in the KR-MCSCF method allows for calculations with large active orbital spaces. Second, using the KR-MCSCF state as a reference point, the CI program is used to treat dynamic correlation based on orbitals which already include the major static correlation and relativistic relaxation in the molecular valence space. The orbital space can now contain up to roughly 120 Kramers pairs, and the CI expansions may be beyond 1×10^8 Slater determinants. Active spaces for the initial KR-MCSCF calculations may now contain more than 50 Kramers pairs. To allow the use of active spaces of this size in conjunction with the high excitation levels typically required to describe static correlation, it is necessary to divide the active orbital space into several subspaces and impose restrictions on the occupations of the various active orbital spaces.

In general, the direct implementations in both the CI and KR-MCSCF methods shift the limitations for KR-MCSCF/CI calculations from memory to CPU time as the rate-determining step. The initial KR-MCSCF implementation[6] is direct in the construction of the energy Hessian matrix and the CI Hamiltonian, removing the memory bottleneck from large-scale applications, but nevertheless becomes inefficient when the configuration spaces exceed about 500 000 Slater determinants. The reason for this is that explicit comparisons of determinants are carried out in the

[a)]Electronic mail: timo@theochem.uni-duesseldorf.de

evaluation of CI coupling coefficients. The new CI module, however, is a genuine string-based implementation where the concept of ordered string graphs[9] is exploited to avoid explicit comparison of strings.

The implementation has been carried out in a local version of the DIRAC04 program package[10] and is a continuation of our methodological work along the lines of relativistic KR-MCSCF/CI for obtaining the wave function and electronic energies. Paper I of this series[11] dealt with the implementation of relativistic double group CI in a two-component framework. Scalar spin-orbitals were used as one-particle functions and the spin-orbit Hamiltonian was represented in the atomic mean-field approximation.[12,13] Paper II (Ref. 8) followed up with a generalization of the CI implementation to the use of Kramers-paired spinors and an interface to the four-component environment.

In the following section on theory and implementation, we review the key features of our relativistic CI method with focus on the issues relevant for implementing large-scale KR-MCSCF. These include the efficient use of generalized active orbital spaces and the implementation of one- and two-electron (transition) density matrices for the active spinors. We next describe the modular incorporation of the CI program in the KR-MCSCF environment. The reader is referred to the preceding papers on direct relativistic CI (Refs. 8 and 11) and KR-MCSCF (Refs. 6, 7, and 14) for further details. In the final section, we apply the new method to the UO_2 molecule. This application illustrates some of the potentials of the new method since much of the novel functionality with respect to construction of active spaces and combining computational approaches is exploited.

II. THEORY AND IMPLEMENTATION

The central new methodological aspects of the implementation presented here are the possibility to carry out relativistic CI and MCSCF calculations with very large CI expansions in an efficient manner and the calculation and use of (transition) one- and two-electron density matrices, both based on relativistic Kramers-paired spinors of double group symmetry (D_{2h}^* and subgroups). In the following subsections, we therefore focus on the ingredients for the required technology, especially in the context of relativistic theory.

A. Relativistic configuration interaction theory

In a recent publication[6] the initial implementation of a Kramers-restricted four-component MCSCF program (KR-MCSCF) for molecules has been presented within a locally modified version of the DIRAC program package.[10] The initial direct second-order implementation employs a CI program which can efficiently handle only up to roughly 500 000 Slater determinants and is therefore limited in applicability. Many typical molecular complete valence space CI expansions surpass this limit, especially since spin-orbit coupling invalidates the use of M_S or S^2 as good quantum numbers. Double point group symmetry may be used without loss of rigor and has been implemented for molecules which have D_{2h} or a subgroup of D_{2h} as point group. The current program version is operational for real matrix groups (D_{2h}^*, C_{2v}^*, and D_2^*) and complex matrix groups (C_{2h}^*, C_2^*, and C_s^*). Quaternion matrix groups (C_i^* and C_1^*) have not been required in application and are therefore not fully debugged.[15]

The introduction of generalized active spaces (GASs) (described in Refs. 11 and 16) replacing the straightforward complete active space (CAS) expansions[17,18] leads to some improvement, because the wave function may be specified by an arbitrary number of active orbital spaces with arbitrary occupation constraints. Nevertheless, most reasonable static correlation GAS expansions exceed 1×10^6 Slater determinants, even for small molecules such as diatomic molecules of heavy elements.

The relativistic double group CI program LUCIAREL described here operates by including all determinants fulfilling the occupation restrictions given by the GAS constraints. The Dirac-Coulomb CI Hamiltonian matrix eigenvalue equation [or for other Hamiltonians of the previous implementations such as the Douglas-Kroll-Hess (DKH) Hamiltonian including mean-field spin-orbit terms[12,13]] is then solved for a specified number of roots in a direct CI fashion in the basis of the generated Slater determinants, thus ensuring simultaneous treatment of dynamic electron correlation and spin-orbit coupling. Recent development work[16] on the program has opened for efficient evaluation of CI (transition) density matrices by the introduction of an excitation class formalism. This procedure maps excitations by grouping them according to the occupation of active (GAS) subspaces and the Kramers barred or unbarred type of the involved creation/annihilation operators in second quantization (details below).

In the GAS concept the various determinants are divided into blocks with each block having given occupations in the various active subspaces. The creator strings are in the same way divided into various occupation types with each occupation type being specified by occupation of the various active orbital spaces.

To show some important features of our implementation we consider the evaluation of sigma vector fragments required in direct CI technology.[9,19] These linear transformations are carried out in basically the same way as the density matrix generation (see Sec. II B 3 and Ref. 8). A sample vector would be

$$\sigma_\mu = \sum_\nu \langle \Phi_\mu | \hat{H} | \phi_\nu \rangle c_\nu \tag{1}$$

expressed in the basis of determinants $|\Phi_\nu\rangle$ and where $\hat{H}$ is the relativistic Hamiltonian[7,11]

$$\hat{H} = \sum_{IJ} \left[h_{IJ}\hat{X}^{+}_{IJ} + \frac{1}{2}(h_{\bar{I}\bar{J}}\hat{X}^{+}_{\bar{I}\bar{J}} + h_{I\bar{J}}\hat{X}^{+}_{I\bar{J}}) \right]$$
$$+ \frac{1}{2}\sum_{KLMN} [(KL|MN)x^{++}_{KLMN}$$
$$+ (\bar{K}\bar{L}|MN)x^{++}_{\bar{K}\bar{L}MN} + (K\bar{L}|MN)x^{++}_{K\bar{L}MN}]$$
$$+ \frac{1}{4}\sum_{KLMN} (\bar{K}L|M\bar{N})x^{++}_{\bar{K}LM\bar{N}}$$
$$+ \frac{1}{8}\sum_{KLMN} [(\bar{K}L|\bar{M}N)x^{++}_{\bar{K}L\bar{M}N} + (K\bar{L}|M\bar{N})x^{++}_{K\bar{L}M\bar{N}}], \qquad (2)$$

expressed in terms of Kramers-paired spinors. Typically, the complete sigma vector cannot be kept in fast memory. It is therefore necessary to divide the σ and C vectors into batches and construct a given batch of the σ vector by reading in batches of the C vector. To construct the σ vector, the C vector may therefore be read in for each batch or more precisely the part of the C vector that contributes to one or more of the blocks of a given batch of σ must be read in. As an increasing number of batches therefore lead to increasing input/output (I/O), it is important to allow as large batches as the available memory allows. An essential part of our division of vectors into batches is the concept of blocks of determinants. Each determinant is defined by a creator string for the occupied unbarred Kramers spinors and a creator string for the occupied barred Kramers spinors: $|\Phi_\nu\rangle = |\mathcal{S}^\dagger_\nu \bar{\mathcal{S}}^\dagger_\nu\rangle$. As already briefly mentioned, the determinants are divided into blocks with each block having given occupations in the various active subspaces. The creator strings are also divided into such occupation types. A given block of determinants is then identified by its Kramers projection value, the occupation types, and the symmetries of the constituent barred and unbarred strings. We then define a batch of determinants as one or several blocks of determinants. The number of blocks in each batch is defined so that the total length of all the blocks in a batch is less than some specified value related to available computer memory. Currently, we typically use 1×10^7. The division of the determinants into blocks and batches does not affect the efficiency as the inner parts of the σ-vector generation from the onset generate the contribution from one block of **C** to one block of σ. The batching of determinants is the most important reason for the lower memory requirements of LUCIAREL compared to the initial KR-MCSCF CI code in DIRAC.[6] Details are again available in the preceding publications.[8,11]

To illustrate the generation of a given block of σ from a given block of **C**, consider the terms from the part of the Hamiltonian that changes the Kramers projection by two units,

$$\sigma^{+2}_{T,\bar{T}} = \sum_{I\geqslant K}\sum_{L\geqslant J}\sum_{\mathcal{S}} \langle T^\dagger|a^\dagger_I a^\dagger_K|\mathcal{S}^\dagger\rangle[(I\bar{J}|K\bar{L}) - (K\bar{J}|I\bar{L})]$$
$$\times \sum_{\bar{\mathcal{S}}} \langle \bar{T}^\dagger|a_{\bar{L}}a_{\bar{J}}|\bar{\mathcal{S}}^\dagger\rangle C_{\mathcal{S},\bar{\mathcal{S}}}, \qquad (3)$$

where $a^\dagger_I$ is a creation operator for an unbarred spinor, $a_{\bar{L}}$ an annihilation operator for a barred spinor, $\mathcal{S}^\dagger$ denotes a string of unbarred creation operators, and $C_{\mathcal{S},\bar{\mathcal{S}}}$ is the CI coefficient for the unbarred/barred string combination $\mathcal{S}^\dagger, \bar{\mathcal{S}}^\dagger$ forming a particular determinant.

As the blocks of σ and **C** are specified, only the part of $\hat{H}$ that connects these two blocks is included. The Hamiltonian is therefore also divided into several sub-Hamiltonians where each sub-Hamiltonian is defined by the changes it produces in the number of the barred and unbarred electrons in each orbital subspace. The blocking of the determinants therefore also reduces the number of integrals that must reside in core at any given time. This is, however, not exploited at the moment. Further details on the evaluation of the σ vector are again available in the preceding publications.[8,11] As a remark on the ongoing work, the division of the determinants into batches allows for a simple fine-grained parallelization of the σ vector evaluation. A batch of coefficients along with the required transformed integrals can be passed to a given processor/node, and after evaluation the various σ vector contributions from the different nodes are kept at the node or gathered to form the complete σ vector.

Another issue worth mentioning in this context is the general implementation of the σ vector evaluation independent of the excitation level of a given determinant with respect to some reference function (e.g., the Dirac-Coulomb Hartree-Fock state). This is possible in genuine string-based algorithms which do not carry out explicit comparisons of configurations/occupations in determining coupling coefficients. LUCIAREL is therefore much more efficient when higher than double excitations are involved than, e.g., the relativistic double group CI code DIRRCI (Ref. 20) that is also included in the DIRAC package.

The previously presented shift to an excitation class formalism in the CI code[8] now opens for the efficient computation of the CI density matrices which are required in a KR-MCSCF optimization. Due to the structural similarity of σ vector and density matrix calculations, this is carried out with the same set of program routines, providing different input and output in the two respective cases. A more detailed description is given in Sec. II B 3.

B. KR-MCSCF implementation

We now turn to the KR-MCSCF implementation and briefly outline the optimization procedure (details may be found in Ref. 6), as the tasks for LUCIAREL immediately become apparent from the derived expressions. The central KR-MCSCF equation system to be solved for a macroiteration step $\boldsymbol{\lambda}^\nu$ reads

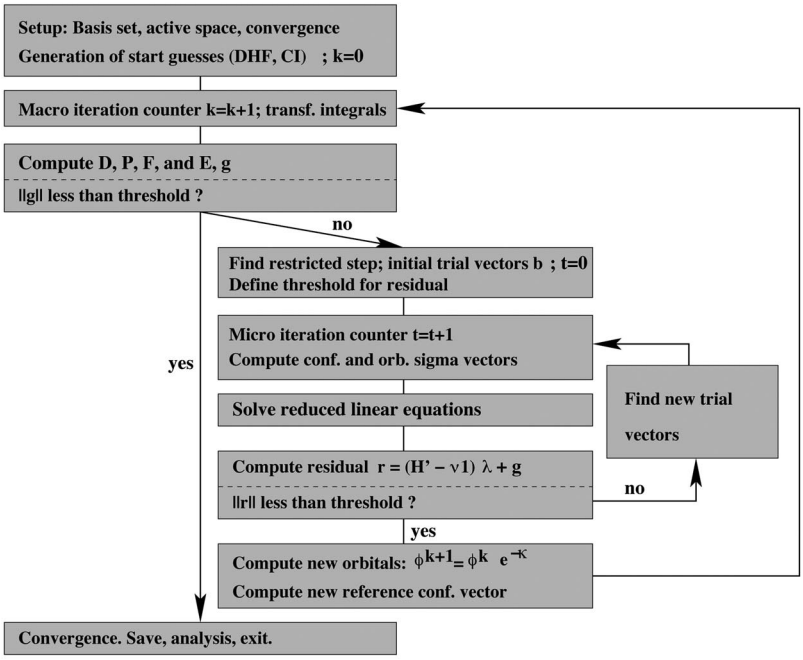

FIG. 1. KR-MCSCF flow diagram. D, P: One- and two-particle density matrices, F: generalized Fock matrix, E: total energy, g: gradient, H: Hessian.

$$\boldsymbol{\lambda}^{\nu} = -(\boldsymbol{E}^{[2]} - \nu \boldsymbol{I})^{-1} \boldsymbol{E}^{[1]} \tag{4}$$

with $\boldsymbol{E}^{[2]}$ is the Hessian matrix, $\boldsymbol{E}^{[1]}$ is the gradient vector, and ν is a level shift parameter evaluated at the current expansion point $\boldsymbol{\lambda}=0$. The Hessian matrix is never calculated explicitly but expanded in a set of trial vectors from which the coefficients are found by solving projected linear equations onto the reduced space of trial vectors

$$\boldsymbol{a}^{\nu} = -(\boldsymbol{E}^{[2R]} - \nu \boldsymbol{I})^{-1} \boldsymbol{E}^{[1R]} \tag{5}$$

with the reduced Hessian and gradient elements,

$$E_{ij}^{[2R]} = \boldsymbol{b}_i^{\dagger} \boldsymbol{E}^{[2]} \boldsymbol{b}_j,$$

$$E_{i}^{[1R]} = \boldsymbol{b}_i^{\dagger} \boldsymbol{R}^{[1]}.$$

The solution $\boldsymbol{\lambda}^{\nu}$ to the full linear equation is found to the required accuracy by means of successive linear transformations

$$\boldsymbol{\sigma}_j = \boldsymbol{E}^{[2]} \boldsymbol{b}_j \tag{6}$$

for a trial vector $\boldsymbol{b}_j$ without setting up the Hessian explicitly. This direct optimization procedure ensures that KR-MCSCF calculations involving a large number of configurational and orbital parameters can be treated. As the Hessian couples orbital and configuration subspaces, the sigma vectors $\boldsymbol{\sigma}_j$ have both orbital and configurational contributions which give rise to different tasks for the CI module. These tasks can be best understood from the program flow diagram given in Fig. 1. To give an overview, we summarize the entry points and their task in Table I before turning to a more detailed discussion in the following Secs. II B 1, II B 2, and II B 3. The top-level routines represent the specific task, the CI start guess, a projection vector (sigma vector) from a given expansion point CI vector, the one- and two-particle density matrices from a given expansion point vector, and finally, if desired, an analysis step of an optimized wave function in configuration space.

1. Start guesses

The setout in a KR-MCSCF macroiteration is a start guess for all optimization parameters, both the occupied Kramers orbitals and the configuration coefficients. The former are determined either by running a Dirac-Coulomb Hartree-Fock SCF calculation or by using a vector from a previous KR-MCSCF run. An initial guess for the CI parameters is gained by transforming the integrals over the Dirac-Coulomb (DC) Hamiltonian to the start guess for the one-particle basis and running a direct CI calculation with a few microiterations only, which is sufficient. This can be understood with the help of the diagram in Fig. 2. The first CI iteration is the initial guess and is the Hartree-Fock determinant in the closed-shell case and a simple linear combination of a few determinants in the open-shell case. Assuming that the initial wave function corresponds to a nonrelativistic or scalar relativistic Hamiltonian, this initial wave function has

TABLE I. The various entry points and tasks for the KR-MCSCF program.

Entry point in LUCIAREL	Needed for
Setup	Number of CI determinants
Configuration interaction	Generation of configuration start guess for KR-MCSCF Any large-scale CI after the KR-MCSCF (Will internally call the "sigma vectors" entry point)
Sigma vectors	Configurational part of gradient Configurational and orbital contribution to configurational sigma vectors
Density matrices	Orbital part of gradient Configurational and orbital contribution to orbital sigma vectors
Configuration vector analysis	Analysis at convergence

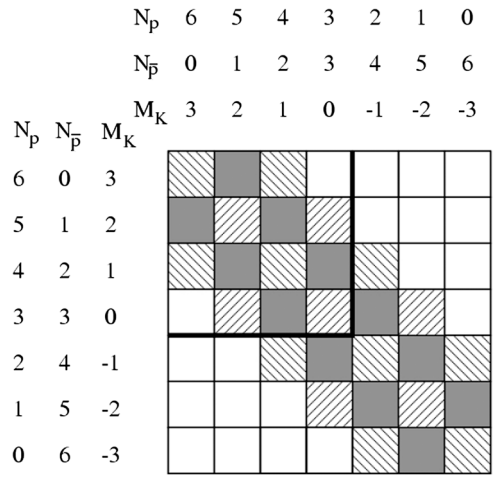

FIG. 2. Coupling diagram for a six-fermion system and the relativistic Kramers-restricted Hamiltonian.

a well-defined Kramers projection value M_K determined from the number of Kramers unbarred (N_p) and barred $(N_{\bar{p}})$ electrons as $M_K=(N_p-N_{\bar{p}})/2$. In the second iteration, all possible couplings from the initial determinants to all singly and doubly excited determinants are included, necessarily having Kramers projection value from M_K to $M_K\pm 2$. This step can be viewed as a first order coupling in terms of perturbation theory. The third iteration includes all the determinants that can be obtained from the initial wave function with up to quadruple excitations and Kramers projection from M_K to $M_K\pm 4$. In the case depicted in Fig. 2 this comprises the full determinant space, but in cases with more open orbitals, a larger number of iterations may be required to include the full determinant space.

An additional feature can be seen from Fig. 2 (further details can be found in Ref. 7): The box in the upper left corner symbolizes the reduction of nonredundant contributions in the case of an even number of electrons. This corresponds to exploiting time-reversal symmetry in the many-particle wave function, the implementation of which would require changes in the linear transformation (sigma vector) evaluations. In the odd-fermion case, time-reversal symmetry is more easily exploited at the many-particle level if Kramers partners fall into different fermion irreducible representations, which is the case in complex matrix groups. Real matrix groups are treated by switching to the highest complex subgroup thus ensuring the same symmetry blocking. Here, in addition, it is exploited that all integrals are purely real.[21]

2. Sigma vector computation

The evaluation of the complete electronic gradient calls for derivatives with respect to the configurational parameters in a given macroiteration. As an example, the term for a determinant $|\Phi_\mu\rangle$ reads [Eq. (3.12) from Ref. 7]

$$\left.\frac{\partial E}{\partial \delta_\mu^*}\right|_{\lambda=0} = \langle \Phi_\mu|\hat{H}|c^{(k)}\rangle - E^{[0]}c_\mu^{(k)}, \tag{7}$$

meaning a sigma-vector-type expression $\hat{H}|c^{(k)}\rangle$ needs to be determined from the current expansion point vector $|c^{(k)}\rangle$.

The second place where computations of sigma vectors are required is in the calculation of orbital and configurational contributions to the configurational Hessian sigma vectors. As described in detail in Refs. 6 and 7, the Hessian matrix is not computed explicitly. Instead, the solution is expanded in a set of trial vectors b in the spinor (o) and configurational (c) space and a complex Davidson algorithm used as update procedure (see, also Sec. II B). One is left with a matrix equation

$$\begin{pmatrix} \boldsymbol{\sigma}^c \\ \boldsymbol{\sigma}^o \\ \boldsymbol{\sigma}^{c^*} \\ \boldsymbol{\sigma}^{o^*} \end{pmatrix} = \begin{pmatrix} \boldsymbol{E}^{[2]c^*c} & \boldsymbol{E}^{[2]c^*o} & \boldsymbol{E}^{[2]c^*c^*} & \boldsymbol{E}^{[2]c^*o^*} \\ \boldsymbol{E}^{[2]o^*c} & \boldsymbol{E}^{[2]o^*o} & \boldsymbol{E}^{[2]o^*c^*} & \boldsymbol{E}^{[2]o^*o^*} \\ \boldsymbol{E}^{[2]cc} & \boldsymbol{E}^{[2]co} & \boldsymbol{E}^{[2]cc^*} & \boldsymbol{E}^{[2]co^*} \\ \boldsymbol{E}^{[2]oc} & \boldsymbol{E}^{[2]oo} & \boldsymbol{E}^{[2]oc^*} & \boldsymbol{E}^{[2]oo^*} \end{pmatrix} \cdot \begin{pmatrix} \boldsymbol{b}^c \\ \boldsymbol{b}^o \\ \boldsymbol{b}^{c^*} \\ \boldsymbol{b}^{o^*} \end{pmatrix}, \tag{8}$$

of which the different elements $E^{[2]c^*c}\cdot b^c$, etc., can be expressed as Eqs. (3.29)–(32) in Ref. 7,

$$\sigma_\mu^{cc} = \langle 0|\hat{H}|B\rangle - E^{[0]}b_\mu^c, \tag{9}$$

$$\sigma_\mu^{co} = \langle \mu|\tilde{H}|0\rangle, \tag{10}$$

$$\sigma_{pq}^{oc} = (\tilde{g}_{pq}^o)^*, \tag{11}$$

$$\sigma_{pq}^{oo} = (\tilde{g}_{pq}^o)^* + \frac{1}{2}\sum_r g(r)b(r), \tag{12}$$

where $\tilde{H}$ and $\tilde{g}$ refer to the one-index transformed Hamiltonian and gradient, respectively, and $g(r)b(r)$ is an abbreviated expression involving products of gradient elements and expansion coefficients.

Again, the first two expressions (9) and (10) correspond to a sigma vector step with the trial vectors $|B\rangle$ (Hessian solution expansion vector) and $|0\rangle$ (current configurational C vector), respectively. The remaining two orbital terms (11) and (12) are derived from the orbital gradient, the evaluation of which will be discussed in the Sec. II B 3.

As an efficient option, integrals with two positronic indices may be neglected in the calculation of sigma vectors. As long as these are included in the gradient, the KR-MCSCF wave function is fully relaxed with respect to electron-positron rotations. Although this is not a fully second-order optimization, it gives satisfactory convergence at a significantly lower cost in the integral transformation.[6,7]

3. Density matrix computations

Both the orbital part of the gradient and of the direct Hessian evaluation require one- and two-particle density matrices over the active space indices (active in the sense of the GAS concept[6]). Excitations between all orbital spaces including the inactive and secondary spaces are included and the spinor gradient element reads

$$\left.\frac{\partial E}{\partial \kappa_{pq}^{*}}\right|_{\lambda=0} = -\langle c^{(0)}|[\hat{X}_{qp}^{-},\hat{H}]|c^{(0)}\rangle = F_{qp} - F_{pq}^{*} = f(\rho_1^{+},\rho_2^{+}). \tag{13}$$

F_{qp} here is a generalized Fock matrix[6,22] and $f(\rho)$ is a function of the one- (ρ_1^+) and two-particle (ρ_2^{++}) density. The introduction of GASs makes the classification of orbital rotations nontrivial. To exclude redundant orbital rotations between two GA orbital spaces, we examine whether the chosen CI space is invariant towards rotations between these two GASs. Redundant orbital rotations are subsequently removed from the parameter space.

In each iteration, the density matrices are constructed to calculate the orbital part of the gradient. The second type of call occurs inside the microiteration loops in the evaluation of the orbital contributions to the orbital sigma vectors. Here, transition density matrices are required for expressions of the type

$$\langle c^{(0,k)}|[\hat{X}_{qp}^{-},\hat{H}]|B\rangle,$$

where B is a trial vector expansion in terms of determinants Φ_μ required for the direct update procedure,

$$|B\rangle = \sum_{\mu} b_\mu |\Phi_\mu\rangle.$$

Exemplifying the calculation of density matrices by analogy to CI sigma vectors (as mentioned in Sec. II A) we discuss the evaluation of a density matrix element for the Kramers flip operator $a_I^\dagger a_K^\dagger a_L a_{\bar{J}}$ of the $\Delta M_K = +1$ class,

$$\rho^{++(r)}(I\bar{J}KL) = \sum_{\mathcal{S},\bar{\mathcal{S}}} \sum_{\mathcal{T},\bar{\mathcal{T}}} \{C_{\mathcal{T},\bar{\mathcal{T}}}^{r} \langle \mathcal{T}^\dagger \bar{\mathcal{T}}^\dagger | a_I^\dagger a_K^\dagger a_L a_{\bar{J}} | \mathcal{S}^\dagger \bar{\mathcal{S}}^\dagger \rangle C_{\mathcal{S},\bar{\mathcal{S}}}^{r} + C_{\mathcal{T},\bar{\mathcal{T}}}^{i} \langle \mathcal{T}^\dagger \bar{\mathcal{T}}^\dagger | a_I^\dagger a_K^\dagger a_L a_{\bar{J}} | \mathcal{S}^\dagger \bar{\mathcal{S}}^\dagger \rangle C_{\mathcal{S},\bar{\mathcal{S}}}^{i}\}, \tag{14}$$

where a real contribution consists of additive real/real and imaginary/imaginary contributions (and likewise for imaginary contributions from real/imaginary and imaginary/real contributions). As described in Ref. 8 the contraction with integrals (in the sigma vector case) is now replaced with a contraction with coefficients. The evaluation procedure is identical, though, and allows for the treatment of any operator in the above form. The calculation of transition densities is easily carried out by replacing the ket vector with the appropriate CI expansion of the reference vectors required in the direct KR-MCSCF steps.

Storage and handling of the generated density matrices are performed via an efficient format which is based on a quaternion representation of the involved quantities.[6,23]

4. Vector analysis

At two stages of the optimization, the CI module may be called for an analysis of the contribution of the various Slater determinants and for the size of the various M_K components. The first stage is after the generation of the configurational start guess, where the analysis provides information about the state one is converging to. The second analysis is invoked at the end of an optimization by passing the final configurational vector to the CI module.

III. APPLICATION: THE UO_2 MOLECULE

The theoretical study of uranium and plutonium compounds is both necessary and interesting, since experiments with hazardous material are costly and often dangerous. Moreover, the plethora of low-lying electronic states in most of the compounds, the influence of spin-orbit coupling, and the importance of electron correlation make computational investigations of high accuracy a difficult task. The UO_2 molecule is an example of an open-shell actinide compound where already the treatment of the ground state is far from trivial. In recent years, several *ab initio* and density-functional theory (DFT) studies of the molecule have been carried out.[24–28]

New experiments[29,30] have allowed for direct comparison with theoretical predictions and facilitated statements about the quality of theoretical results. The recent REMPI experiments of Han *et al.*[30] confirm previous theoretical work that predicts UO_2 to be linear and symmetric in its ground state. Two open-shell electrons form an *ungerade* manifold of low-lying states arising from the $U(5f\,7s\sigma_g)O_2$ configuration and a *gerade* manifold from the $U(5f^2)O_2$ configuration. The most recent calculations employed the complete active space second-order perturbation theory (CASPT2) combined with spin-orbit coupling at the complete active space state interaction level[31] (in the following called SO-CASPT2) and spin-orbit CI calculations performed with the COLUMBUS program package[32] using relativistic effective core potentials. In these studies, the lowest states are predicted to be of ungerade symmetry and are characterized as $\Omega=2u$ and $\Omega=3u$. These states have, as dominant components, determinants obtained by populating the $U(7s\sigma_g)$ and $U(5f_{5/2})$ spinors in a j-j-coupling picture. In an LS-coupling scheme this latter spinor corresponds to the nonbonding $U(5f_\phi)$ orbital that lies slightly below the also nonbonding $U(5f_\delta)$ orbital.

The splitting between the lowest u and g states is of interest because the shifts in the asymmetric stretch vibrational frequency going from a neon to an argon matrix, that were observed by Zhou *et al.*,[33] may be explained by assuming a change of ground state in the argon matrix. This viewpoint is supported by the theoretical work of Li *et al.*[26] which indeed indicates a significant lowering of the gerade states upon coordination with argon. This interaction could be strong enough to cause a matrix-induced change of ground state, similar to the one observed in CUO.[34] This explanation is, however, not in agreement with the electronic spectra of UO_2 in argon reported by Heaven and co-workers.[29,30] These spectra make an assignment of the ground state as gerade unlikely. In a recent paper Gagliardi *et al.*[28] presented new calculations and concluded that although theoretical calculations cannot rule out the change of ground state, this is not very likely given the good agreement of the observed electronic spectra with the gas-phase computational data.

To give a first indication of the results that can be obtained using a consistent treatment of both scalar and spin-orbit relativistic effects, we will investigate the lowest u and g states of UO_2 in terms of their character and excitation energy, both vertical and adiabatic. At the KR-MCSCF level,

TABLE II. The symmetry and main contribution of the active spinors in the UO_2 KR-MCSCF calculation. Bonding orbitals are denoted in boldface.

Gerade	Ungerade
$7s(U)\ \sigma^*$	$\{5f(U)\}\ \{7p(U)\}$
$7s(U)\ \sigma$	
$2p(O)\ \pi$	$\mathbf{2}p(\mathbf{O})\mathbf{5}f(\mathbf{U})\ \boldsymbol{\sigma}$
$2p(O)\ \pi$	$\mathbf{2}p(\mathbf{O})\mathbf{5}f(\mathbf{U})\ \boldsymbol{\pi}$
$\mathbf{2}p(\mathbf{O})\mathbf{6}d(\mathbf{U})\ \boldsymbol{\sigma}$	$\mathbf{2}p(\mathbf{O})\mathbf{5}f(\mathbf{U})\ \boldsymbol{\pi}$

the calculations will be carried out with sufficiently large active spaces and CI expansions to allow for the description of static correlation. As dynamic electron correlation has a profound impact on the spectroscopic properties of this system, we investigate the ground state and the excited states by applying GASCI based on both Dirac-Coulomb Hartree-Fock (DC-HF) and KR-MCSCF spinors. These calculations serve to analyze the bonding situation and will shed light on the interplay of spin-orbit (SO) coupling and electron correlation that is of crucial importance to make a reliable prediction of the precise ordering of the u and g states.

A. DC-HF and KR-MCSCF calculations

The calculations have been performed using the uncontracted basis sets from Ref. 35 with $\{26s21p17d12f\}$ functions on uranium and $\{10s5p2d1f\}$ functions on oxygen and at various internuclear distances along the linear symmetric stretch coordinate of the molecule in the D_{2h}^* double group symmetry. The initial set of molecular spinors is obtained from a DC-HF calculation with state averaging over the $7s^15f^1(u)$ double open-shell configuration. The selection of active spaces for the subsequent KR-MCSCF calculations requires a characterization of the molecular spinors. This is done by Mulliken population analysis and by determining the $\hat{L}_z$ expectation values of the spinors in question and assigning (approximate) projection quantum numbers λ. The $\hat{L}_z$ analysis reveals that almost all of the Kramers pairs are close to an integer λ value; therefore spin-orbit coupling has only a minor influence at the one-particle level. This concerns both the bonding orbitals (where one $\sigma-\pi$ mixing occurs) and the virtual-space orbitals. Consequently, we obtain in essence the same bond lengths when running the DC-HF calculation with and without spin-orbit terms ($R_e=3.314a_0$ including and $R_e=3.315a_0$ neglecting spin-orbit coupling). The averaging over configurations carried out in the DC-HF is not the reason for this, as this averaging only includes nonbonding orbitals.

The active KR-MCSCF space is composed as given in Table II. The active space contains the energetically highest occupied DC-HF Kramers pairs from the averaged calculation, four of which are bonding. We include the entire set of $5f(U)$ and $7p(U)$ functions as they are partially mixed and cannot be separated unambiguously. In addition, an antibonding gerade function is included.

A CASSCF calculation with the 14 valence electrons in these 18 Kramers pairs yields a configuration space of roughly 1×10^9 determinants, a calculation which is feasible but too time consuming. We have tested two different restricted active space calculations. The first includes all excitations up to triples in the active space (SDT, 143 330 determinants), the second up to pentuples (SDTQ5, 15 200 032 determinants). We use an odd maximum excitation level because the ground state is expected to be singly excited with respect to the closed-shell reference setup. The larger space thus contains up to quadruple excitations out of the ground state. The KR-MCSCF calculations are approximated by neglecting rotations between positive energy and negative energy orbitals, i.e., freezing the no-pair partitioning to that of the DC-HF calculation. This approximation has a negligible effect on the computed energies.

TABLE III. Dominant contribution to $5f_\phi$ and $5f_\delta$ for various forms of spinor optimization.

Oribital type	DC-HF	KR-MCSCF SDT	KR-MCSCF SDTQ5
$5f_\phi$	$86\%\,\phi$, $14\%\,\delta$	$90\%\,\phi$, $10\%\,\delta$	$90\%\,\phi$, $10\%\,\delta$
$5f_\delta$	$95\%\,\delta$, $5\%\,\pi$	$86\%\,\delta$, $14\%\,\pi$	$70\%\,\delta$, $30\%\,\pi$

We find the $2u$ state as the lowest state from the u manifold in both the smaller and the larger KR-MCSCF calculations. With the SDT setup, a potential curve has been calculated yielding an equilibrium bond distance of $R_e=3.348a_0$, a bond elongation compared to the average of configuration DC-HF result of $R_e=3.314a_0$. This comparison of a state energy with an average energy expression is meaningful because the averaging in the DC-HF is carried out over the nonbonding $5f(U)$ and $7p(U)$ spinors and should give a reasonable first guess of the bond distance in the ground state. Restricting the open-shell occupation in the DC-HF to $7s(U)\sigma_g\ 5f(U)\phi$ leads to a bond length of $R_e=3.312a_0$, in accord with our arguments. The lowest g state is obtained by a corresponding KR-MCSCF calculation at a single point, $3.481a_0$, as $4g$ for which the excitation energy is 0.669 eV. The g states are known to have minima at significantly longer bond distances than the u states,[25] however. An adiabatic excitation energy including dynamic electron correlation is necessary to obtain a result reliable enough to make a more definite statement about the true excitation energy of the gerade states that are assumed to be significantly lowered in energy in argon matrices.

A Mulliken population analysis and $\hat{L}_z$ analysis of the spinors reveal that the correspondence between the SDT and SDTQ5 KR-MCSCF states is good. The g orbitals do not undergo any significant change. Some variation in the form of the $5f_\phi$ and $5f_\delta$ spinors on the form of spinor optimization is observed as reported in Table III. The character of these two active orbitals determines to a large degree the excitation energies to the lowest excited states. Despite the increasing π character of the δ-type orbital with the correlation level, we consider the smaller KR-MCSCF calculation a reasonable starting point for dynamic correlation calculations, because all internal excitations of the KR-MCSCF SDTQ5 calculations are included in the MRCI calculations.

B. Multireference CI calculations

MRCI calculations using LUCIAREL will be carried out to investigate two aspects of the electronic states of the UO_2

TABLE IV. Equilibrium bond lengths and adiabatic excitation energies of low-lying electronic states of UO_2 using SDT KR-MCSCF orbitals (MC) or DC-HF spinors (DC-HF) and comparison with experiment and other approaches.

	T_e (cm^{-1})		R_e (a_0)		
State	Present	Expt.[a]	Present	SO-CASPT2[b]	SOCI (COLUMBUS)[c]
$2u$	0	0	3.372	3.375	3.401
$3u^{MC}$	417	360	3.379		
$3u^{DC\text{-}HF}$	···		3.375		

[a]Reference 30.
[b]Reference 24.
[c]Reference 25.

molecule. First, we want to determine a precise bond length of the $2u$, $3u$ states by using state-specific SDT KR-MCSCF ($2u$) spinors as one-particle basis. This will also yield the adiabatic excitation energy of the (expected) first excited state $3u$. Second, we will run single-point calculations for a larger number of excited states in both the g and u symmetries at different correlation levels and compare with other methods and experiment.

1. Potential curves

The configuration space for these calculations is based upon the KR-MCSCF SDT reference expansion and all single and double excitations into a virtual space truncated at 2 a.u., amounting to 44 virtual Kramers pairs and a total expansion length of almost 1×10^7 determinants. States were identified (also in Sec. III B 2) by comparing small CAS CI calculations with identical runs using the DIRAC module DIRRCI (Ref. 20) which can exploit linear symmetry and directly delivers the Ω quantum numbers.

The results are compiled in Table IV. All presented methods find $2u$ as the ground state also at the correlated level. The adiabatic excitation energy for the $3u$ state is in good agreement with experiment, given the small splitting between the two states. The bond lengths hardly differ for the $2u$ and $3u$ states and the two curves are nearly parallel. Using DC-HF spinors, this correspondence is even better as the averaging eliminates the state-specific (here $2u$) character of the orbitals in the (MC) calculation. Finally, we find excellent agreement between our value and the SO-CASPT2 result if we take the result obtained with a similar basis set and active CASSCF space as ours. The deviation with the SOCI result obtained with the COLUMBUS program is somewhat larger. This deviation has two possible sources. We use—for reasons of feasibility—a truncation of the virtual space. We do not expect, however, that increasing the size of the virtual space would lead to a significantly different equilibrium bond length. The SOCI calculation on the other hand has been carried out only at the SDCI level and uses an effective core potential.

2. Excited states

Vertical excitation energies are determined by single-point calculations at a U–O separation of $3.481a_0$ which is between the u and g state minima. All calculations are based on averaged $7s^15f^1(u)$ DC-HF spinors except where noted otherwise. For purposes of comparison we determine the excitation energies at different levels of electron correlation. CAS2 denotes a CASCI calculation with the two-open-shell electrons only. S12C2-SD stands for a run with single excitations from the six doubly occupied Kramers pairs into a CAS2 space and single and double excitations into the virtual space (now truncated at 5 a.u.) from the complete reference space. The SDT-SD space is the same as in Sec. III B 1 but now also with a truncation value of 5 a.u. This largest calculation includes nearly 23×10^6 Slater determinants.

Results for the states of u symmetry are collected in Table V. At all levels, $2u$ is the molecular ground state. Already the two-electron CAS calculation reproduces the states in the correct ordering and even with reasonable excitation energies. Adding on the 12 electrons in an intershell correlation type of model space reduces the excitation energies somewhat. The fully correlated level brings the energies back to the CAS2 results. This indicates that differential electron correlation is quite small for these plain-valence calculations. The $3u$ excitation energy derived with MC spinors is seen to be poorer than the DC-CI value, implying that state averaging in the orbital optimization is to be preferred in DC-CI calculations of excited states.

When comparing to other methods and experiment, the difference in U–O separation needs to be accounted for. The

TABLE V. Excitation energies of u electronic states of UO_2 at different correlation levels and comparison with experiment and other approaches. S12C2-SD denotes single (S) excitations of 12 valence electrons, a CAS with two electrons in the U($7s,7p,5f$) orbitals and single and double (D) excitations into the virtual space from all reference determinants so created. SDT-SD denotes SDT excitations from seven occupied valence orbitals to the U($7p,5f$) orbitals and a σ_g^* orbital and SD excitations into the virtual space from all reference determinants so created. The CV-SDT-SD calculation has been carried out with an augmented basis set.

State	CAS2	S12C2-SD	SDT-SD$^{(MC)}$	SDT-SD	SDT-SD	CV-SDT-SD ($+3g1h$)	SOCI (COLUMBUS[a])	SO-CASPT2[b]	Expt.
$2u$	0	0	0	0	0	0	0	0	0[c]
$3u$	477	416	518	460	427		431	378	360[c]
$1u$	1416	1336		1478	1089		1088	2567	*1094*[d]
$2u$	1853	1763		1922	1542	2042	1566	2908	*1401*[d]
$4u$	5904								
U–O Separation	$3.418a_0$	$3.481a_0$	$3.481a_0$	$3.481a_0$	$3.372a_0$	$3.372a_0$	$3.402a_0$	$3.452a_0$	

[a]Reference 25.
[b]Reference 28.
[c]Reference 30.
[d]Reference 29.

SO-CASPT2 energies are computed at $3.452a_0$, the SOCI values at $3.402a_0$. Shifting our most elaborate potential curve down to the shorter SOCI bond distance results in close agreement of the CI approaches. For better comparison, we have also carried out a single-point calculation at our minimum bond distance of $3.372a_0$. The agreement between these excitation energies and the SOCI (COLUMBUS) energies is remarkable, and both methods give excitation energies very close also to the matrix experimental values (given in italics in Table V). The SO-CASPT2 results which are very close to the gas-phase experiment in case of $3u$ are off by more than 1000 cm^{-1} for the excited states $1u$ and $2u$. By deeper analysis, we attempt to answer two questions that arise. (1) What is the possible source for the deviation of the SO-CASPT2 results from all other values for the $1u$ and $2u$ excited states? (2) Is the close agreement between the two SOCI values and the matrix experiment substantiated or coincidental?

Considering the second question first, we extend our correlation treatment to include excitations from the subvalence orbitals to obtain excitation energies of greater reliability for the gas-phase molecule. We do this by opening the $2s$(O) and $6p$(U) for single excitations in a core-valence type of correlation manner, combined with the reference space from the plain-valence calculation correlating 14 electrons. In total, 24 electrons are correlated yielding a configuration space of more than 50×10^6 determinants. The SO-CASPT2 method treats ten electrons as active and the additional 14 electrons by perturbation theory, so the correlation levels are now at better balance for a comparison. Our calculation has only been carried out for the irreducible representation containing the two $2u$ states, and the obtained excitation energy is 1814 cm^{-1}. Thus, the excitation energy increases by roughly 270 cm^{-1} compared to the valence calculations. The preliminary results of four-component coupled cluster calculations on UO_2 (Ref. 36) also give an increasing $2u$ excitation energy upon correlating 24 electrons. Obviously, the excitation energy is not converged with respect to the treatment of electron correlation at the plain-valence level.

To further increase the accuracy of our calculation, we augmented the basis set by functions of high angular momentum, $3g$ and $1h$ function, essentially for correlating the uranium f electrons (exponents 2.725 913 629, 0.861 203 1602, and 0.365 998 661 6 for g and 1.604 319 77 for h). The recalculated $2u$ excitation energy is now increased to 2042 cm^{-1} (denoted CV-SDT-SD in Table V), a substantial correction of another 228 cm^{-1}. The coupled cluster calculation conducted by Infante and Visscher[36] using the same basis set indicates that including double excitations from the uranium $6p$ shell will lead to another increase of this excitation energy as compared to our final value of 2042 cm^{-1}.

Turning to the first question now, the SO-CASPT2 value we compare has been obtained vertically at a different bond length but at the minimum geometry obtained with that correlation treatment. Even if we shift along the potential curves to bring the U–O separation to agreement, the variance in excitation energy is not more than 200 cm^{-1}, because the respective potential curves are nearly parallel. There are two other theoretical possibilities for the deviation. The SO-CASPT2 calculations are carried out using spin-orbitals instead of spinors as one-particle basis. An analysis would require running our respective calculations with spin-orbitals in the two-component implementation of LUCIAREL.[8] We do not believe, however, that the use of spinors can make up for such large a difference in excitation energies, given our results from Sec. III A. The last possibility concerns the assumption of additivity of spin-orbit coupling and dynamic electron correlation in the SO-CASPT2 approach. Simulating this kind of treatment is not possible with our current implementation. It remains to be shown whether an additive treatment of spin-orbit coupling and electron correlation can deviate from the simultaneous treatment on such a scale for excitation energies of lower excited states.

TABLE VI. Excitation energies of g electronic states of UO_2 at different correlation levels and comparison with other approaches. S12C2-SD denotes single (S) excitations of 12 valence electrons, a CAS with 2 electrons in the U($7s$,$7p$,$5f$) orbitals and single and double (D) excitations into the virtual space from all reference determinants so created.

State	SO-CASPT2[a]	S12C2-SD^{DF-HF}
$4g$	3 330	3 102
$0g(s^2)$	···	5 862
$1g$	6 823	7 243
$2g$	12 073	11 648
U–O separation	$3.452a_0$	$3.481a_0$

[a]Reference 28.

We gain confidence from our calculations that the true $2u$ excitation energy must be larger than 2000 cm^{-1}. This is corroborated by the other mentioned approaches. Therefore, either the differential matrix effect on the experimental result in Table V is tremendous or the experimental assignment of the excited state is in error. A conclusive judgment would be premature at this stage, and we leave the issue for further investigation.

Table VI shows our results for the lowest set of g states, calculated at the intershell correlation level and compared to SO-CASPT2. The same ordering of states is found and the excitation energies are in good agreement for the $4g$ and $2g$ states after shifting along the potential curve. For the $1g$ state a deviation of at least 600 cm^{-1} remains. The $0g$ state from the $7s^2$(U) configuration is found as the second vertically excited state of g symmetry and was not calculated in Ref. 28. Due to the small intensities for the $7s$ to $5f$ excitation these states have not been observed so that we cannot verify the accuracy of the calculation by comparing with experiment. Given the reasonable agreement with the SO-CASPT2 values, we may in this case assume that differential correlation is small and that the computed energies comprise reasonable predictions of the excitation energies. Without explicitly calculating the $UO_2\cdot Ar$ interaction energies it remains, however, impossible to predict whether the lowest of these states may fall below the $2u$ state in an argon matrix.

IV. SUMMARY AND OUTLOOK

We present a four-component relativistic direct KR-MCSCF/CI program system capable of performing calculations with large active orbital spaces and configuration spaces. Relativistic contributions, in particular, spin-orbit coupling, are treated simultaneously with electron correlation in both the KR-MCSCF and the post-MCSCF CI step. For computational feasibility, approximations such as the neglect of electron-positron orbital rotations, or integrals with two positronic indices in the calculation of sigma vectors giving satisfactory convergence at a significantly lower cost in the integral transformation, can be invoked. The program system opens for the efficient and precise calculation of spectroscopic properties of heavy-element molecules with arbitrary shell structures in ground and excited states.

The initial application concerns the UO_2 molecule. In agreement with recent other studies and gas-phase experiments, we find $\Omega=2u$ as the molecular ground state and the same ordering of the lowest excited states of g and u symmetries. The effect of spin-orbit coupling at the orbital optimization level is found to be small, especially on the bonding molecular Kramers pairs. This is reflected by the very small bond contraction of only $0.001a_0$ when comparing a spin-orbit free and a full relativistic calculation. We determine a U–O bond length of $R_e=3.372a_0$ when including static and dynamic electron correlations and spin-orbit coupling fully variationally. The single-point excited state calculations reveal that differential electron correlation is rather small at the valence-correlated level including 14 active electrons. This changes upon including excitations from the subvalence shells, where the excitation energy of the $2u$ state increases by 270 and by 500 cm^{-1} upon augmenting the basis set in addition. This finding also indicates that the reported excitation energies from argon matrix experiments could differ by up to 0.1 eV from the corresponding gas-phase values if they have been correctly assigned. A final statement on the molecular ground state in a rare-gas matrix cannot be made. In comparison with other methods, we find an error cancellation for excitation energies when correlating too few electrons. Our results suggest that a simultaneous treatment of electron correlation and spin-orbit coupling in quantum chemical studies is required for obtaining high-precision (errors smaller than 0.05 eV) excitation energies of UO_2.

We are proceeding with a work on improvement and extension of the available methodology. Parallelization of the CI program is highly desirable for greater efficiency on modern computers with many processors and large amounts of shared memory. The integral transformation step in the KR-MCSCF procedure, the time-consuming step in smaller configuration space applications, is already parallelized. Current work involves exploiting that all integrals are real in the real matrix double groups $(D_{2h}^*, D_2^*, C_{2v}^*)$ (Refs. 6 and 21) which concern all linear molecules and a large fraction of nonlinear small molecules. Furthermore, the linear symmetry implementation in the DIRRCI program will be utilized also for LUCIAREL, which will greatly facilitate calculations on linear molecules. With respect to spectroscopic properties, the access to transition moments would be of great desire. One of the next steps will therefore be to make use of our already implemented transition densities between different CI vectors to calculate transition moments for direct comparison with experiment.

Concerning further studies, we are investigating diactinide compounds, in particular, the U_2 molecule. In these systems spin-orbit coupling is likely to be of much greater importance than in UO_2, and a fully relativistic treatment yielding Kramers-paired spinors would shed further light on the bonding picture in such systems. The above-mentioned implementational improvements will then also reduce the computational demand and facilitate the interpretation of obtained data.

We conclude that our presented four-component relativistic direct KR-MCSCF/CI method is a significant and useful new tool for electronic structure calculations on small heavy-element molecules. To further increase the reliability of the dynamic electron correlation treatment, we are also extending LUCIAREL by merging it with a new multireference coupled cluster (MRCC) method[37,38] opening for Kramers-restricted MRCC treatments. Based on KR-MCSCF wave functions, this method will allow for coupled cluster calculations on heavy-element molecules with an arbitrary number of open shells.

ACKNOWLEDGMENTS

One of the authors (T.F.) would like to acknowledge a research scholarship from the Deutsche Forschungsgemeinschaft (DFG), Grant No. FL 356/1-1, and thank the University of Southern Denmark (Odense) for hospitality. This work was also supported by the Danish Natural Science Research Council, Grant No. 21-02-0467, and a grant of computer time by the John von Neumann Institute for Scientific Computing (NIC) at the Forschungszentrum Jülich (Germany).

[1] B. A. Heß and C. M. Marian, in *Computational Molecular Spectroscopy*, edited by P. Jensen and P. R. Bunker (Wiley, Sussex, 1999).
[2] *Handbook on the Physics and Chemistry of Rare Earths*, edited by K. A. Gschneidner Jr. and L. Eyring (Elsevier Science, New York, 1996), Vol. 22, Chap. 152, pp. 1–116.
[3] *Encyclopedia of Computational Chemistry*, edited by P. von Ragué Schleyer (Wiley, New York, 1997), pp. 1–11.
[4] Z. Zhang and R. M. Pitzer, J. Phys. Chem. A **103**, 6880 (1999).
[5] G. A. Bishea and M. D. Morse, J. Chem. Phys. **95**, 5646 (1991).
[6] J. Thyssen, H. J. Aa. Jensen, and T. Fleig, J. Chem. Phys. (submitted, under revision).
[7] H. J. Aa. Jensen, K. G. Dyall, T. Saue, and K. Fægri, J. Chem. Phys. **104**, 4083 (1996).
[8] T. Fleig, J. Olsen, and L. Visscher, J. Chem. Phys. **119**, 2963 (2003).
[9] J. Olsen, B. O. Roos, P. Jørgensen, and H. J. Aa. Jensen, J. Chem. Phys. **89**, 2185 (1988).
[10] Dirac, a relativistic *ab initio* electronic structure program, Release DIRAC04.0 (2004), written by H. J. Aa. Jensen, T. Saue, L. Visscher, with contributions by V. Bakken, E. Eliav, T. Enevoldsen *et al.*, (http://dirac.chem.sdu.dk).
[11] T. Fleig, J. Olsen, and C. M. Marian, J. Chem. Phys. **114**, 4775 (2001).
[12] B. A. Heß, C. M. Marian, U. Wahlgren, and O. Gropen, Chem. Phys. Lett. **251**, 365 (1996).
[13] B. Schimmelpfennig, AMFI, an atomic mean-field spin-orbit integral program, University of Stockholm, 1996 and 1999.
[14] T. Fleig, C. M. Marian, and J. Olsen, Theor. Chem. Acc. **97**, 125 (1997).
[15] For details on the specification of matrix groups see, e.g., Ref. 23.
[16] T. Fleig, Habilitationsschrift, Mathematisch-Naturwissenschaftliche

Fakultät, Universität Düsseldorf, 2006.
[17] B. O. Roos, P. Taylor, and P. E. M. Siegbahn, Chem. Phys. **48**, 157 (1980).
[18] P. E. M. Siegbahn, J. Almlöf, A. Heiberg, and B. O. Roos, J. Chem. Phys. **74**, 2384 (1981).
[19] J. Olsen, P. Jørgensen, and J. Simons, Chem. Phys. Lett. **169**, 463 (1990).
[20] L. Visscher, T. Saue, W. C. Nieuwpoort, K. Fægri, and O. Gropen, J. Chem. Phys. **99**, 6704 (1993).
[21] L. Visscher and T. Saue, J. Chem. Phys. **113**, 3996 (2000).
[22] J. Thyssen, dissertation, Department of Chemistry, University of Southern Denmark, 2001.
[23] T. Saue and H. J. Aa. Jensen, J. Chem. Phys. **111**, 6211 (1999).
[24] L. Gagliardi, B. O. Roos, P.-Å. Malmqvist, and J. M. Dyke, J. Phys. Chem. A **105**, 10602 (2001).
[25] Q. Chang, thesis M.S., Graduate School, The Ohio State University, 2002.
[26] J. Li, B. E. Bursten, L. Andrews, and C. J. Marsden, J. Am. Chem. Soc. **126**, 3424 (2004).
[27] C. Clavaguéra-Sarrio, V. Vallet, D. Maynau, and C. J. Marsden, J. Chem. Phys. **121**, 5312 (2004).
[28] L. Gagliardi, M. C. Heaven, J. W. Krogh, and B. O. Roos, J. Am. Chem. Soc. **127**, 86 (2005).
[29] C. J. Lue, J. Jin, M. J. Ortiz, J. C. Rienstra-Kiracofe, and M. C. Heaven, J. Am. Chem. Soc. **126**, 1812 (2004).
[30] J. Han, V. Goncharov, L. A. Kaledin, A. V. Komissarov, and M. C. Heaven, J. Chem. Phys. **120**, 5155 (2004).
[31] P.-Å. Malmqvist, B. O. Roos, and B. Schimmelpfennig, Chem. Phys. Lett. **357**, 230 (2002).
[32] S. Yabushita, Z. Zhang, and R. M. Pitzer, J. Phys. Chem. **103**, 5791 (1999).
[33] M. Zhou, L. Andrews, N. Ismail, and C. Marsden, J. Phys. Chem. A **104**, 5495 (2000).
[34] J. Li, B. E. Bursten, B. Liang, and L. Andrews, Science **295**, 2242 (2002).
[35] W. A. D. Jong, L. Visscher, and W. C. Nieuwpoort, J. Mol. Struct.: THEOCHEM **458**, 41 (1999); **581**, 259(E) (2002).
[36] I. Infante and L. Visscher (private communication).
[37] J. Olsen, J. Chem. Phys. **113**, 7140 (2000).
[38] J. W. Krogh and J. Olsen, Chem. Phys. Lett. **344**, 578 (2001).